

# MOMENT TENSOR ANALYSIS OF MIDDLE AND LARGE EARTHQUAKES IN NICARAGUA

**Petronila Guadalupe Flores Ayerdis\***  
**MEE12606**

**Supervisor: Bunichiro SHIBAZAKI\*\***

## ABSTRACT

We determined moment tensor solutions for middle and large-size earthquakes that occurred during the period 1990-2013 in the subduction zone, Nicaraguan forearc and Nicaraguan depression, using inversion analysis of teleseismic waveforms. In order to understand tectonic stress state from the subduction zone to the inland crust in Nicaragua, we estimated stress drop for each earthquake using obtained values of seismic moment and half duration of source time function. We found that the thrust faulting is clearly predominant in subduction zone, generating shallow earthquakes with magnitudes up to more than Mw 7, while in the Nicaraguan forearc the faulting type is mixed including thrust and strike-slip faulting, generating intermediate earthquakes with magnitudes between Mw 5.3-6.9. On the other hand, in Nicaraguan depression the strike-slip faulting with left-lateral motion is predominant, generating shallow earthquakes with magnitudes between Mw 5.3-6.1. Then, we examined the relationship between seismic moment and half duration of source time function, and found that the stress drop for each earthquake is nearly constant between 0.1-10 MPa with no dependence on seismic moment. Earthquakes with a depth of 50-100 km show higher stress drop than earthquakes with a depth of 0-50 km. Our results give information for understanding of tectonics in Nicaragua.

**Keywords:** Moment Tensor Inversion, Seismic Moment, Stress Drop, Nicaragua

## 1. INTRODUCTION

Occurrence of earthquakes is affected by the stress field in a region induced by movement of tectonic plates and the subsequent deformation field. Nicaragua is located in the western border of the Caribbean plate, between the Cocos, North American and South American plates, constituting a very complex region, which is characterized by being exposed to extensional and compressional stresses. Such stresses are caused by the interaction between the Caribbean and Cocos plates.

As a result of the plate motions, in Nicaragua the seismic activity is concentrated along the subduction zone, Nicaraguan forearc sliver and Nicaraguan depression, considering the subduction zone as the most seismic active area. However, the seismic activity generated along the Nicaraguan depression has caused inland earthquakes highly devastating of up to Mw 6.3 as was experienced in 1972.

In this study we investigate moment tensors for earthquakes located in the subduction zone, Nicaraguan forearc sliver and Nicaraguan depression, to present new insights about stress field in Nicaragua. We use a program set developed by Yagi and Nishimura (2011) to obtain moment tensor solutions by inversion analysis of seismic waveforms for middle and large-size earthquakes that occurred during the period 1990-2013. We also estimate the stress drop for middle and large-size earthquakes. Obtained results will give essential information for understanding of tectonics in Nicaragua.

---

\*Institute of Geology and Geophysics, National Autonomous University of Nicaragua (IGG-CIGEO/UNAN-Managua).

\*\*International Institute of Seismology and Earthquake Engineering (IISEE), BRI, Japan.

## 2. DATA

In this study, we analyzed only teleseismic body waves (P-waves) from 41 events for a period from 1<sup>st</sup> January 1990 to 30 June 2013 in the range of latitude between 10.65°N and 15.1°N and longitude between -89°W and -82°W with moment magnitude (Mw) above 5.



Figure 1. Location map of GSN broadband and US array backbone stations (IRIS-DMC Network).

We obtained waveform data through Wilber II application from the Data Management Center of the Incorporated Research Institution for Seismology (IRIS-DMC) via the Internet. Figure 1 shows an example of the GSN broadband station and US array backbone station distributions from a viewpoint of good azimuthal coverage with distance range from 30° to 90°.

## 3. THEORY AND METHODOLOGY

### 3.1. Moment Tensor Inversion

Recently, inversion techniques have been developed using the broadband seismic waveform, from which the synthetic seismograms are compared with observed seismograms applying iterative techniques to determine earthquakes parameters. We used the program set developed by Yagi and Nishimura (2011) for estimating moment tensor solutions.

Hereafter we explain the method of inversion following the paper by Yagi and Nishimura (2011). In general, the observed seismic waveform of  $c$  component at a station  $j$  due to the seismic moment release in a source volume  $V$  is given by

$$u_{cj}(t) = \sum_{q=1}^6 \iiint_V \tilde{G}_{cj}(\mathbf{r}, \xi) * \tilde{M}_q(t, \xi) d\xi + e'_{cj}(t), \quad (1)$$

where  $\tilde{G}$  is the Green's function of basis moment tensor (Kikuchi and Kanamori, 1991),  $\tilde{M}$  is a spatio-temporal moment density function, and  $e'$  is an observed error. Since the volume change during earthquakes is too small to detect, we can neglect the volume change component  $\tilde{M}_6$ . To estimate stable moment tensor solutions, we should assume a simple source model such as the point source model, in which we assume the seismic waveform to be radiated from one point. Following the point source model, we rewrite Eq. (1) as

$$u_{cj}(t) = \sum_{q=1}^5 \tilde{G}_{cj}(\mathbf{r}, \xi_c) * \tilde{M}_q(t) + e_{cj}(t), \quad (2)$$

with

$$M_q(t) = \iiint_V \tilde{M}_q(t, \xi) d\xi, \quad (3)$$

where  $\xi_c$  is the location of the centroid, and  $e$  contains observed and modeling errors. We assumed that the focal mechanism is kept constant during an earthquake, and approximated the shape of the source time function to be an isosceles triangle with half duration of  $t_r$ . Based on the assumption of the constant focal mechanism and the simple source time function, we can rewrite Eq. (2) as

$$u_{cj}(t) = \sum_{q=1}^5 m_q \times G_{cj}(\mathbf{r}, t_r, \xi_c) + e_{cj}(t), \quad (4)$$

with

$$G_{cj}(\mathbf{r}, t_r, \xi_c) = \tilde{G}_{cj}(\mathbf{r}, \xi_c) * T(t, t_r), \quad (5)$$

where  $T$  is a source time function with half duration of  $t_r$ . In general, we apply low-pass filters to observed data for mitigating the aliasing effect in re-sampling procedure, the effect of the complicated seismic source process and the effect of the heterogeneity of the local velocity structure. Therefore, relationship between the observed seismic waveform and data waveform is represented by

$$d_{c_j}(t) = B(t) * u_{c_j}(t) \quad (6)$$

where  $B$  is the function of the low-pass filter. Substituting Eq. (4) into (6), we then rewrite in the following simple vector form:

$$\mathbf{d} = \mathbf{A}(t_r, \xi_c) \mathbf{m} + \mathbf{e} \quad (7)$$

where  $\mathbf{d}$  and  $\mathbf{e}$  are  $N$ -dimensional data and error vectors, respectively;  $\mathbf{m}$  is a 5-dimensional model parameter vector;  $\mathbf{A}$  is a  $N \times 5$  coefficient matrix. The solution of the above matrix equation is obtained by the least square approach if we assume the duration of the source time function  $t_r$  and the centroid location  $\xi_c$ . Also, we assumed that the horizontal location of the centroid can be approximated to the epicenter, estimated optimal depth of the centroid and half duration using the grid-search method, which minimizes normalized L2-norm as  $\|\mathbf{d} - \mathbf{A}(t_r, \xi_0) \mathbf{m}\| / \|\mathbf{d}\|$ .

### 3.2. Stress Drop

Stress drop is one of the most important parameters in the description of earthquake source properties. This parameter is determined by the source size and seismic moment. In order to evaluate the stress drop, we assume a circular crack model. Using the Brune's formula that relates seismic moment  $M_o$  and stress drop  $\Delta\sigma$ :

$$M_o = \frac{16}{7} \Delta\sigma a^3 \quad (8)$$

where  $a$  is the radius of the fault, which is assumed to be expressed using rupture velocity  $V_r$  and source duration  $t_d$ :

$$a = V_r t_d \quad (9)$$

Substituting Eq. (9) into (8), we obtain

$$M_o = \frac{16}{7} \Delta\sigma (V_r t_d)^3 \quad (10)$$

Therefore, stress drop can be estimate as

$$\Delta\sigma = \frac{7}{16} \frac{M_o}{(V_r t_d)^3} \quad (11)$$

where  $V_r$  is assumed to be 2.5 km/s.

## 4. RESULTS

### 4.1. Moment Tensor Inversion

Using a program set developed by Yagi and Nishimura (2011), we analyzed 41 earthquakes from 1990 to 2013 to obtain moment tensor inversion of seismic waveforms and find out the best depth and source time with the minimum variance. We determined moment tensor for 30 events,

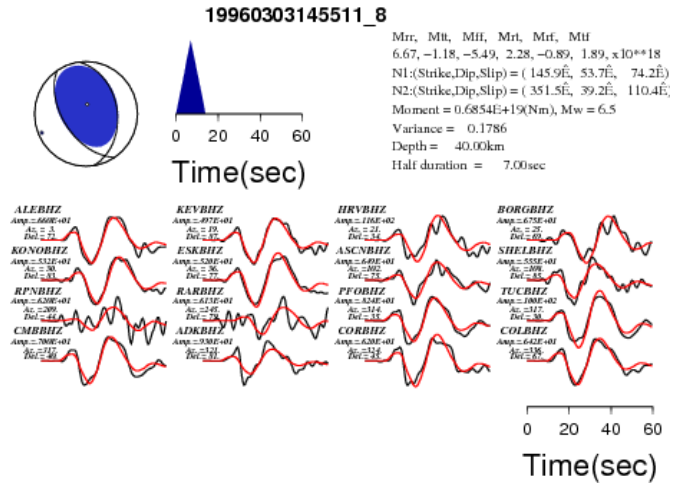


Figure 2. Example of moment tensor solutions obtained for the 1996 March 03 Mw 6.5. Upper left and middle figures show the focal mechanism and the source time function of the solution. Upper right shows information of source parameters. Lower figures show observed (black lines) and synthetic (red lines) waveforms.

because the waveforms of the others events did not have good S/N ratio to obtain solutions. Figure 2 shows an example of a solution for the 1996 March 03 event with Mw 6.5.

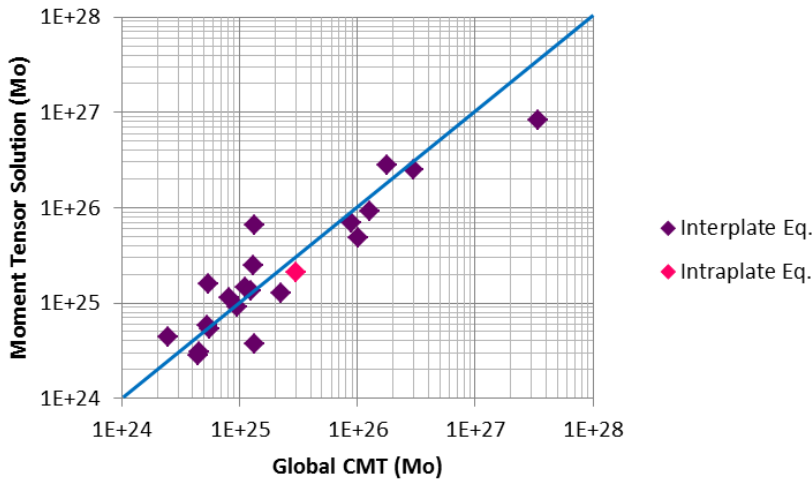


Figure 3. Comparison of seismic moments (dyne-cm) between obtained moment tensor solutions and Global CMT solutions based on type of earthquakes.

features of the tectonic setting in Nicaragua and suggest that a large number of earthquakes show moment tensor solutions clearly dominated by thrust faulting, in some cases varying their mechanism to oblique thrust and low-angle thrust faulting (Figure 4). This type of faulting produces shallow earthquakes (0-50 km) and deep earthquakes (80-130 km) with moment magnitudes up to more than 7 (purple circle in Figure 5), which are generated due to subduction process between the Cocos and Caribbean plates, proving that the subduction zone is the most seismic active area in Nicaragua.

According to historical records the 1992 Nicaragua tsunami earthquake is the event with larger magnitude occurred in the subduction zone, which corresponds with the larger earthquake analyzed in this study (92/09/02 in Figure 5). The magnitude of the 1992 earthquake is Mw 7.2 in our solution although that of Global CMT is Mw 7.6. This may be due to the method using body waves in our analysis.

As is dominant in the subduction zone, the seismic events generated show thrust faulting with exception of some events for example the 1996 March 27 and 2004 April 28 events that show normal faulting. These earthquakes are located very near to the Middle America Trench (96/03/27 and 04/04/28 in Figure 4).

A moderate number of the earthquakes are located in the Nicaraguan forearc. These earthquakes show moment tensor solutions that include interplate earthquakes with thrust faulting and intraplate earthquakes with strike-slip faulting (Figure 4). These types of faulting generate intermediate earthquakes (30-70 km) with moment magnitudes between 5.3 and 6.9 (green diamond in Figure 5), which are generated as a consequence of the subduction of the Cocos plate beneath the

We compare the obtained seismic moments and those of GCMTs (Figure 3) and we found that obtained seismic moments are generally consistent with those of Global CMT results. However, some seismic moments of our results were different from those of Global CMT; one of the reasons is that we used body waves although Global CMT is determined using long-period waves.

We plotted the focal mechanisms obtained in this study and we found that the moment tensor solutions demonstrate the different

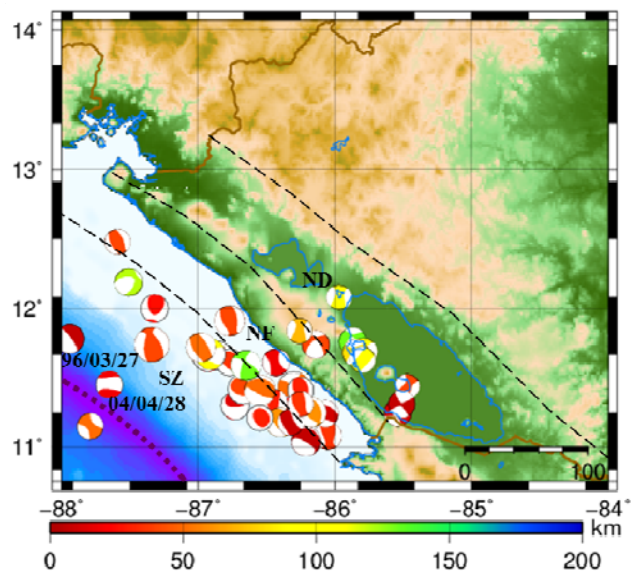
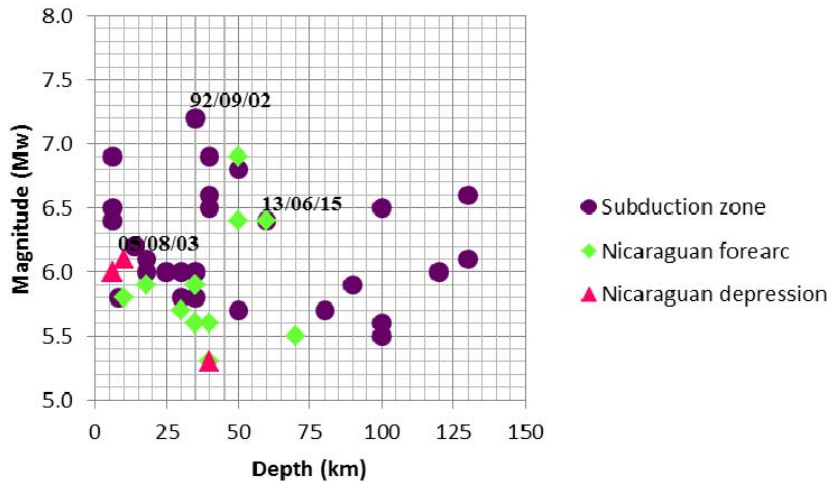


Figure 4. Focal mechanism solutions of moment tensor inversion. Abbreviations: SZ-Subduction Zone; NF-Nicaraguan Forearc; ND-Nicaraguan Depression.

Caribbean plate; however it also includes the local faulting system along the Pacific coast of Nicaragua.

The largest historical earthquake in this zone occurred in 1956 and it had a magnitude of Mw 7.3. In this study the 2013 June 15 event is considered to be the largest earthquake with a moment



magnitude of Mw 6.4 (13/06/15 in Figure 5).

Finally, a few number of earthquakes show moment tensor solutions represented by strike-slip faulting, with left-lateral motion mainly along the Nicaraguan depression (Figure 4). This type of faulting generates shallow earthquakes (0-40 km) with moment magnitudes between 5.3 and 6.1 (pink triangle in Figure 5).

Figure 5. Relationship between moment magnitude and depth of obtained moment tensor solutions based on type of faulting.

In this area, highly devastating inland earthquakes have occurred historically, with magnitude up to Mw 6.3

as was experienced in 1972. In this study, the 2005 August 03 event is considered to be the largest shallow inland earthquake within the Nicaraguan depression (05/08/03 in Figure 5).

#### 4.2. Stress Drop

From equation (10), we obtain the following equation:

$$\log M_o = 3 \log t_d + \log \frac{16}{7} \Delta \sigma V_r^3 \quad (12)$$

We examined the relationship between  $\log M_o$  and  $\log t_d$  as shown in Figure 6. Three blue lines indicate cases with stress drop of 0.1, 1 and 10MPa and types of faulting are also indicated. We found that  $\log M_o$  is in proportion to  $\log t_d$  and stress drops range from 0.1MPa to 10MPa, namely there is no systematic dependence of stress drop on seismic moment. As can be seen in Figure 6, some strike-slip earthquakes show high stress drops with ranges between 1MPa and 10MPa. These events are intermediate depth earthquakes. Thrust earthquakes show a clear tendency that  $\log M_o$  is in proportion to

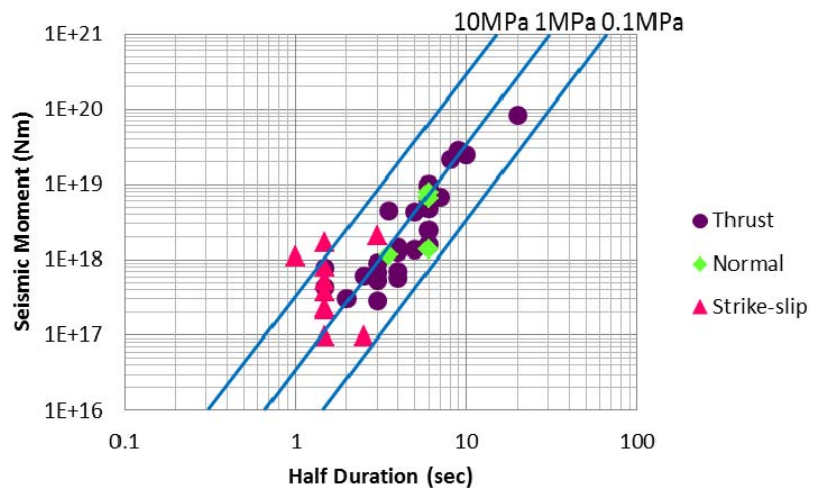


Figure 6. Relationship between seismic moment and half duration of obtained moment tensor solutions based on type of faulting and stress drop.



$\log t_d$ .

We also examined the relationship between the seismic moment and half duration with different depth ranges (Figure 7) and we found that stress drop of intermediate depth (50-100 km) earthquakes are larger than those of shallow depth earthquakes (Figure 7).

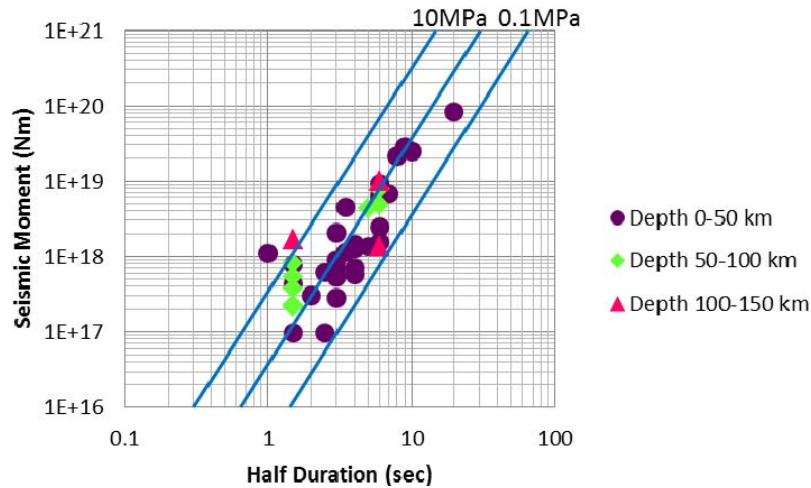


Figure 7. Relationship between seismic moment and half duration of obtained moment tensor solutions based on classification of depth and stress drop.

in centroid depth and seismic moments between our results and Global CMT solutions, which may be due to the difference in method for determining moment tensors.

Regarding moment tensor solutions obtained in this study, the thrust faulting is clearly predominant, generating shallow earthquakes with moment magnitude up to more than 7 in the subduction zone, while in the Nicaraguan forearc the faulting are mixed including thrust and strike-slip faulting that generate intermediate earthquakes with moment magnitudes between 5.3 and 6.9. On the other hand, in Nicaraguan depression the strike-slip faulting with left-lateral motion is predominant, generating shallow earthquakes with moment magnitudes between 5.3 and 6.1.

Using Brune's formula we estimated stress drop for each earthquake, which is nearly constant between ranges from 0.1MPa to 10MPa. From these results we found no dependence of stress drop on seismic moment but an increase of stress drop with depth.

It is necessary to work more with this methodology to obtain a better understanding of the tectonic setting and tectonic stress field for subduction earthquakes and inland earthquakes around Nicaragua.

## 5. CONCLUSIONS

To determine the behavior of middle and large-size earthquakes in Nicaragua, we obtained moment tensor solutions in and around Nicaragua. We used the program set developed by Yagi and Nishimura (2011) for determining moment tensor solutions using teleseismic waveforms. We obtained solutions of 30 events from 1990 to 2013. We compared the results with the solutions from Global CMT. Some differences are seen

## ACKNOWLEDGEMENTS

I am extremely thankful to Professor Yuji YAGI (Tsukuba University) who kindly provided me the program and technical guidance for moment tensor analysis.

## REFERENCES

- Kikuchi, M., and Kanamori, H., 1991, Bull. Seism. Soc. Am., Vol. 81, No.6, pp. 2335-2350.
- Madariaga, R., 1979, Journal of Geophysical Research, Vol. 84, No. B5, pp. 2243-2250.
- Ruff, L.J., 1999, Pure and Applied Geophysics, v. 154, pp. 409-431.
- Yagi, Y., and Nishimura, N., 2011, Bull. of Inter. Inst. of Seism. and Earthq. Eng., 45, pp. 133-138.